Proceedings of the 2006 IEEE/RSJ
International Conference on Intelligent Robots and Systems
October 9 - 15, 2006, Beijing, China

Haptic Simulation for Micro/Nano-Scale Optical Fiber Assembly

Qi Luo and Jing Xiao

IMI Lab, Department of Computer Science
University of North Carolina - Charlotte
Charlotte, NC 28223, USA
{*qluo, xiao*}*@uncc.edu*

***Abstract*— While there are very high industry demands on optical fiber, little research has been done on the modeling and simulation of the optical fiber assembly. In this paper, the interaction forces in the micro/nano joining step of the optical fiber assembly are modeled. Simulation of assembly in a virtual environment via a haptic device is performed, and experimental results are discussed, which could be used for designing leaning-based controller for automated micro/nano-scale optical fiber assembly.**

I. Introduction

Demands for optical fiber is very high in communications industry. optical fiber is a particularly popular technology for local-area networks, and telephone companies are steadily replacing traditional telephone lines with optical fiber cables. It is predicted that almost all communications in the future will employ optical fiber.

However, optical fiber assembly is very complicated due to many technical challenges [1]. optical fiber is very thin at the scale of $100\mu m$ and is vulnerable to damages caused by bending, kinking and crushing during assembly. Its assembly is subject to complex nano-scale adhesive forces but requires extremely high precision. Little is done to analyze and understand the force effects and physical properties during optical fiber assembly. As the result, more than 75% of optical fiber components are currently assembled manually, which is very tedious, inefficient, and often leads to damaged products.

This paper is motivated by the need to automate optical fiber assembly in order to achieve high efficiency and high product quality. We provide an analysis of the different nano-scale adhesive forces as well as the contact force present during optical fiber assembly and establish proper force models. Based on the models, we further simulate the nano-scale process during optical fiber assembly in a virtual environment with haptic rendering. The results could be useful for improving optical fiber assembly and facilitating eventual automation of the process.

While simulation and virtual prototying is useful in product design and manufacturing in general, it is particularly crucial for manufacturing at micro/nano-scale [2] [3] [4]. Unlike normal-scale operations, visual feedback (through microscopes) for nano-scale operations can include many sources of errors, and real force feedback cannot be felt at the nano-scale (in the range of 0.1 up to 200 μN). There is no force sensor or measuring device that can be used on the fiber to detect forces at this scale. There is also limited understanding of the fundamental physics of nano-scale objects and their interactions. Proper simulation of nano-scale operations in a virtual setting with scaled up forces can help providing the necessary visual and especially force feedback to human operators for the design and testing of nano-scale operations and products. It further facilitates automation of nano-scale operations.

Existing work in micro/nano-scale simulation is mainly focused on operations using atomic force microscope (AFM) nano-probes or scanned probe microscope (SPM) [3] [5] [6] [7], where a nano-scale object is touched or manipulated by a very sharp tip mounted on a flexible cantilever. As far as we know, there is little research concerning the modeling and simulation of optical fiber assembly, which this paper is focused on.

The rest of the paper is organized as follows. In section II, we describe the scope of simulation of the optical fiber assembly process in this paper. In Section III, we analyze and present related force models. In Section IV, we describe haptic simulation and discuss results. We conclude the paper in Section V.

II. Simulation Scope of Assembly Process

The three major steps in optical fiber assembly process are the preparing for production, the joining and the positioning. Fiber preparation is the first step in the assembly process. It typically includes stripping the outer jacket of the fiber, cleaning and cleaving the fiber, and polishing the end of the fiber. Since these operations are normal-scale operations and do not require very high precision, they are relatively easy to be performed fully automated with no operator intervention. On the other hand, the joining and positioning steps usually require the accuracy to be better than several microns (1 micron = 10^{-6} meter) to achieve efficient coupling and positioning.

In the joining step, a major process is to insert the fiber into the ferrule that locates inside the connector (Fig. 1). As shown in Fig. 2, the ferrule on the connector is a long, thin,

1-4244-0259-X/06/$20.00 ©2006 IEEE

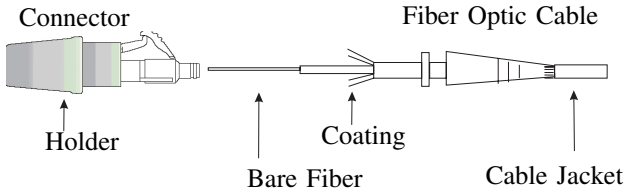

Fig. 1. Inserting optical fiber into an ST connector's ferrule

hollow cylinder which acts as a fiber alignment mechanism. Ferrules are typically made of metal or zirconia ceramics, but they may also be constructed of plastic.

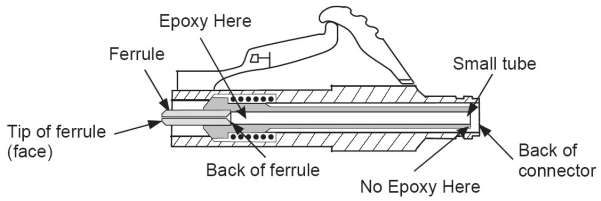

Fig. 2. Cross-sectional view of a connector [8]

Since the ferrule's inner diameter is $\phi = 126$ microns, and the diameter of the bare fiber (which consists a core and its outside cladding) is $\phi = 125$ microns, the insertion of the fiber into the ferrule occurs at micro/nano-meter scale. The fiber's physical properties undergo many significant changes at such a small scale. Micro/Nano-mechanisms need to be used for studying force or motion of the fiber. Adhesion force and other short-ranged surface forces cannot be omitted. Friction force at this scale also acts differently from the friction force under normal scale due to the increased surface-to-volume ratio. During the insertion, these interactive forces between the fiber and the ferrule may damage the fiber and decrease the transparency of the fiber. Therefore, understanding the optical fiber insertion operation is one of the key elements in a successful optical fiber assembly.

In this paper, we focus on force modeling during fiber-ferrule insertion and haptic simulation of the process.

III. Micro/Nano-Scale Force Modeling

In this section, we first present existing force models for micro/nano-scale manipulations, then we introduce force models specifically for the fiber-ferrule insertion process. Both contact and non-contact forces are modeled. Effects of different forces are compared and discussed.

A. Existing Contact Force Models

There are several existing models of adhesion forces for the simulation of the contact mechanics at micro/nano-scale [9], such as Hertz model, Johnson-Kendall-Roberts (JKR) model, Derjaguin-Muller-Toporov (DMT) model and Maugis-Dugdale (MD) model. When the external loads are much greater than the adhesion forces, the Hertz model is realistic. If the load amounts have similar magnitudes to adhesion forces, adhesion force effect should be taken into account. The DMT model can be used in the case of rigid systems, low adhesion and small radii of curvature, but it may underestimate the true contact area. JKR model includes the adhesion force effect while assumes that the short-ranged surface forces act only inside the contact area. The MD model, developed from all above models, is a more appropriate solution that does not underestimate surface forces and contact area.

In modeling micro/nano-scale manipulations, friction force is often not considered.

B. Existing Research with Non-Contact Force Modeling

When one object approaches another object and the distance between them is at micro/nano-scale, there are many non-contact forces [10] between the objects, including van der Waals force, which is the intermolecular force that deal with forces due to the polarization of molecules, electrostatic force, which is a long-range force arising between static electric charges, and capillary force, which may be caused by high humidity conditions within the manufacturing environment or immersion and removal from a liquid, in addition to gravity force.

Existing research on modeling micro/nano-manipulations is mostly focused on the interaction between the tip of an AFM or SPM nano-probe and a nano-scale object. Formulae are presented for computing many non-contact forces, such as van der Waals force [11], electrostatic force [3], capillary force [4] [12] [13]. Gravity force is ignored due to the nano-scale sizes of both the tip and the object.

C. Our Approach

Unlike the tip-object interaction considered in the existing research, in optical fiber-ferrule insertion, the interaction region between the fiber and the ferrule is much larger. Therefore, the existing formulae for non-contact forces cannot be directly applied here. We extended the existing approaches by taking into account the changeable interaction region during insertion, the epoxy layer that may be formed inside the ferrule, and the shape of the interaction region between the fiber and the ferrule.

We adopt the MD model to represent the contact adhesion force, since it is the only model that does not underestimate surface forces and the contact area. In addition, gravity force becomes much more significant due to the micro-scale radius of the fiber and cannot be ignored. We also consider friction force using the Hurtado and Kim (HK) model, which is a micromechanical model that provides an expression for the behavior of the friction stress over the wide range of contact areas [14].

Below, we list some common geometric parameters used in our force models, some of which are also illustrated in Fig. 3 and Fig. 4.

h: minimum distance between the fiber and the ferrule
l_f: segment length of the fiber inside the ferrule

r: radius of the fiber
l_b: length of the manipulated segment of the fiber
θ: angular range of the interaction region between the fiber and the ferrule (see Fig. 3)
S: interaction area between the fiber and the ferrule: $S = r\theta l_f$

D. Non-Contact Force Models for Fiber-Ferrule Insertion

When the distance h between the optical fiber and the ferrule inner surface is down to less than $100nm$, van der Waals force becomes significant. Electrostatic force and gravitational force also plays an important role. In addition, the capillary force is not negligible in some cases as the result of certain joining techniques.

Since the gap h can be treated as between two planar regions due to the very small gap-to-radius ratio ($|h|/|r| << 1$) (see Fig. 3), the van der Waals force can be computed as

$$F_{vdw} = -\frac{HS}{24\pi h^3} \qquad h \leq 100nm \tag{1}$$

where the *Hamaker constant* H is dependent on the material properties of the boundaries, e.g., for metals, it is about several $10^{-19}J$.

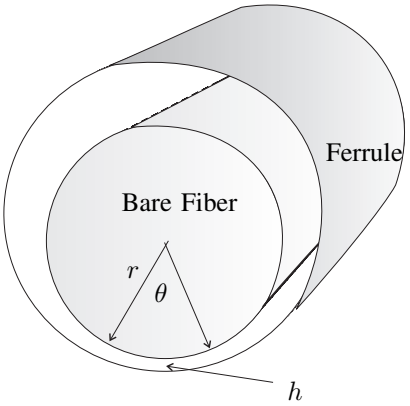

Fig. 3. The cross-section of the optical fiber deviating from the center of the ferrule

The electrostatic force can be computed as

$$F_{el} = -\frac{\epsilon_0 U^2 S}{2h^2} \qquad h \geq a_0 \tag{2}$$

where ϵ_0 is the permittivity, U and a_0 are the resulting voltage difference and the interatomic distance between the fiber and the ferrule, respectively.

The gravitational force for the manipulated portion of the optical fiber can be calculated as

$$F_{grav} = \rho_{s_i} \pi r^2 l_b \tag{3}$$

where ρ_{s_i} is the density of silicon.

When the optical fiber is jointed by adhesives or soldering, a liquid layer is formed between the lower surface of the fiber and the inner surface of the ferrule, as shown in Fig. 4. Due to the relatively large interaction region between the fiber and the ferrule, the capillary force is no longer negligible and can be expressed as

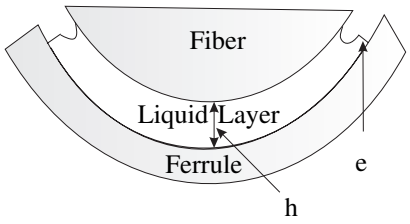

Fig. 4. The cross-section of the liquid layer formed between the optical fiber and the ferrule

$$F_{cap} \approx -2\gamma_L l_f (1 - \frac{h - 2e}{2r_1}) \cos\theta_c \tag{4}$$

where θ_c is the contact angle of the meniscus, e is the thickness of the liquid layer, γ_L is the liquid surface energy, and r_1 can be calculated as $h/(2\cos\theta)$.

The directions of F_{vdw}, F_{el}, and F_{cap} are along the minimum distance between the fiber and the ferrule. The total non-contact force $\vec{F}_{nc}$ is the sum:

$$\vec{F}_{nc} = \vec{F}_{vdw} + \vec{F}_{el} + \vec{F}_{grav} + \vec{F}_{cap} \tag{5}$$

E. Contact Forces Models for Fiber-Ferrule Insertion

Once a contact is formed between the fiber and the ferrule, to reduce the risk of damage on the optical fiber, one should try to break the contact. To do so, the force $\vec{F}_c$ that needs to be exerted on the fiber should overcome the adhesion force from the inner surface of the ferrule and the friction force if the break-away direction is not normal to the the contacting surface, in addition to overcoming the gravity.

Since the forces exerted on the optical fiber and the ferrule are relatively small, both the fiber and the ferrule act relatively rigidly to the loads exerted on them. To make the case simple, we can assume that the radius a of the contact area has a linearly changed value ($100nm \sim 120nm$) corresponding to a very small range of penetration depth ($0 \sim 10nm$) once contact happens.

Using the MD model, we can compute the adhesion force F_{ad} as

$$F_{ad} = \frac{Ka^3}{r} - \lambda a^2 (\frac{\pi\varpi K^2}{r})^{1/3} (\sqrt{m^2 - 1} + m^2 \arctan\sqrt{m^2 - 1}) \tag{6}$$

where ϖ is the work of adhesion evaluated at contact, $\varpi \approx 2\gamma_L$ when a thin liquid layer exists between the surfaces of the fiber and the ferrule. m is the *non-dimensional adhesion radius* which is $m = c/a$, c is the extent of the adhesion zone on the radial direction. λ is a dimensionless parameter, for MD model, its value should satisfy $0.12 < \lambda < 5.8$. K is so called *reduced elastic modulus* with the value can be calculated from

$$\frac{1}{K} = \frac{3}{4}((\frac{1 - \nu_o^2}{E_o}) + (\frac{1 - \nu_f^2}{E_f})) \tag{7}$$

where E_o, E_f, and ν_o, ν_f are *Young's moduli* and *Poisson ratios* of the optical fiber and the ferrule.

The friction force at micro/nano scale acts differently from the normal scale friction force as the contact area between the fiber and the ferrule is in the order of μm. It can be computed as

$$\frac{F_{fric}}{G^* b^2} = \begin{cases} \bar{\tau}_{f_1} \bar{a}^2 & \bar{a} < \bar{a}_1 \\ 10^B \bar{a}^{M+2} & \bar{a}_1 < \bar{a} < \bar{a}_2 \\ \bar{\tau}_{f_2} \bar{a}^2 & \bar{a} > \bar{a}_2 \end{cases} \quad (8)$$

where the *non-dimensional contact radius* $\bar{a} = a/b$ is a normalized by the *Burgers vector magnitude* b [15], and the *non-dimensional friction stress* $\bar{\tau}_f$ is the *friction stress* τ_f normalized by the *effective shear modulus* $G^* = 2G_1G_2/(G_1 + G_2)$, where G_1 and G_2 are the shear moduli of the contacting bodies. The constants M and B of Eq. 8 are given by

$$M = -\frac{\log(\bar{\tau}_{f_1}/\bar{\tau}_{f_2})}{\log(\bar{a}_2/\bar{a}_1)} \quad (9)$$

$$B = \frac{\log(\bar{\tau}_{f_1})\log(\bar{a}_2) - \log(\bar{\tau}_{f_2})\log(\bar{a}_1)}{\log(\bar{a}_2/\bar{a}_1)} \quad (10)$$

$\bar{a}_1 \approx 50$, $\bar{a}_2 \approx 10^5$, $\bar{\tau}_{f_1} \approx 0.02$, and $\bar{\tau}_{f_2} \approx 8 \cdot 10^{-4}$.

The total contact force is

$$\vec{F}_c = \vec{F}_{ad} + \vec{F}_{fric} \quad (11)$$

F. Effects of Different Forces

Table. I gives a set of typical values for the parameters that are used in the force models described above. Based on these data, the forces can be simulated and compared.

TABLE I
PARAMETERS USED IN SIMULATION

P	Value	P	Value
$H(J)$	$(3.67 \pm 0.02) * 10^{-19}$ [a]	$\gamma_L(mJ/m^2)$	72 [b]
$\theta_c(^\circ)$	60	$e(nm)$	80
$\epsilon_0(C^2/Nm^2)$	$8.85 * 10^{-12}$	$U(V)$	0.1
$\rho_{s_i}(Kg/m^3)$	2330 [c]	$\theta(^\circ)$	90
$a_0(nm)$	0.1	$E_0(Kg/m^2)$	$4.7 * 10^{10}$ [c]
ν_0	0.35 [c]	$E_f(Kg/m^2)$	$7.0 * 10^{10}$ [a]
ν_f	0.35 [a]	m	1.05
$l_b(cm)$	5.0	$b(nm)$	0.48
$G_1(Kg/m^2)$	$3.17 * 10^9$ [c]	$G_2(Kg/m^2)$	$0.73 * 10^9$ [a]
λ	4.0		

[a]Parameter of aluminum
[b]Parameter of water
[c]Parameter of silicon

Fig. 5 compares the magnitudes of the van der Waals force (F_{vdw}), the capillary force (F_{cap}), the electrostatic force (F_{el}), and the gravity force (F_{grav}) as the functions of the minimum distance h between the fiber and the ferrule. h is small enough but non-zero. The gravity force drags the optical fiber downward while the other forces attract the fiber towards the inner surface of the ferrule. The capillary force and the gravity dominate in the given case, while the electrostatic force and the van der Waals force are negligible. However, when optical fiber is jointed by laser welding, no liquid layer is formed between the surface of fiber and the inner surface of the ferrule; hence the capillary force does not exist, and the van der Waals force becomes significant especially when the minimum distance between the fiber and the ferrule is smaller than $10nm$.

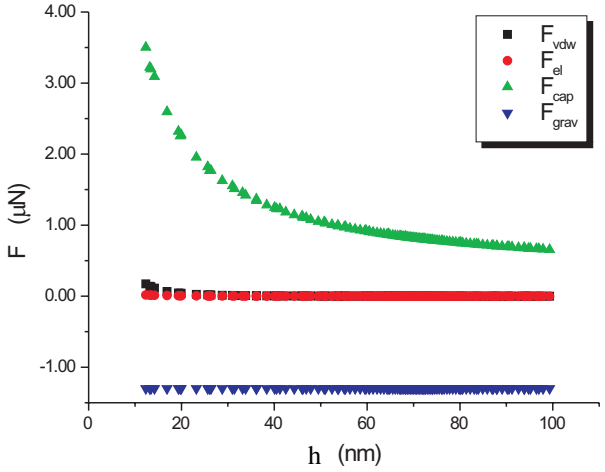

Fig. 5. Magnitudes of the simulated non-contact forces vs. the minimum distance between the fiber and the ferrule

Fig. 6 shows the non-contact forces linearly increase as the insertion deepens, i.e., the length of the inserted optical fiber segment increases.

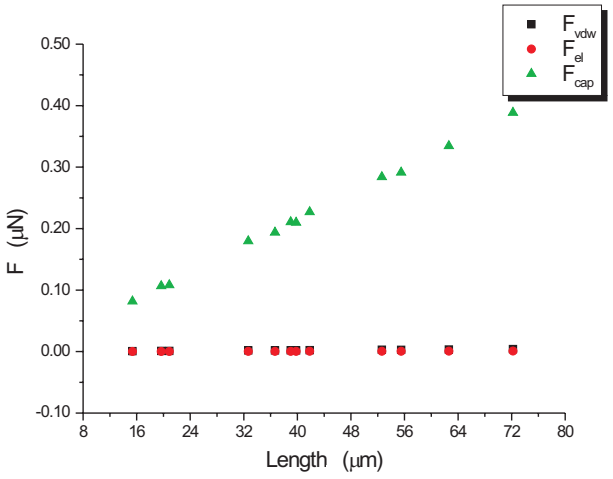

Fig. 6. Magnitudes of the non-contact forces vs. the inserted length of the fiber segment

When a contact happens between the ferrule and the fiber, the adhesion force (F_{ad}) first acts as an attractive force but

then quickly becomes an increasingly repulsive force as the penetration depth d increases, as shown in Fig. 7.

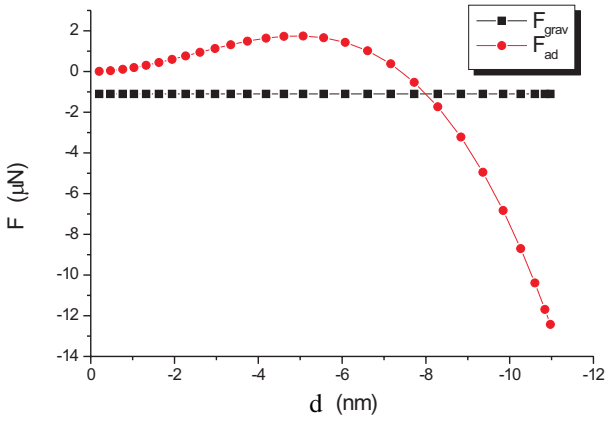

Fig. 7. Magnitudes of forces vs. the penetration depth when a contact happens

IV. Haptic Simulation and Experiment

We have simulated the fiber-ferrule insertion process based on the force models developed in a virtual environment with real-time haptic rendering via a PHANToM Premium 1.5/6DOF device and a personal computer with dual Intel Xeon 2.4GHz processors and 1GB system RAM. The human operator can virtually hold the simulated optical fiber through the haptic device and insert the fiber into the simulated fixed ferrule.

We first describe how the micro/nano scale task is magnified for simulation and then present some experimental results.

A. Scaling Control

To simulate the fiber-ferrule assembly task, the micro/nano-scale contact or non-contact forces have to be magnified to be forces at the normal scale so that they can be felt by a human operator via a haptic device. The micro/nano-scale object displacements also need to be magnified. The scaling factors have to be set taking into account stability and fidelity.

In this paper, micro/nano-forces and displacements are set as linearly scaled with constants α_f and α_x similar to those in [3]:

$$F_s = \alpha_f F_m \tag{12}$$

$$X_s = \alpha_x X_m \tag{13}$$

where F_m and X_m are the force and displacement in real assembly task at micro/nano-scale, F_s and X_s are the corresponding force and displacement of F_m and X_m in the virtual world at the normal scale.

The scheme of the scaling control is shown in Fig. 8.

The scaling factors α_x and α_f can be set by the heuristic rule as

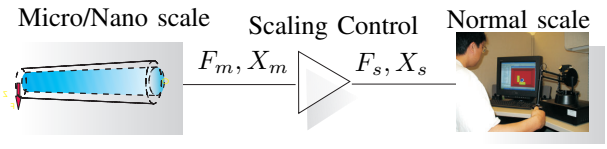

Fig. 8. Overview of scaling control

$$\alpha_x = \frac{x_s^{max} - x_s^{min}}{x_m^{max} - x_m^{min}} \tag{14}$$

$$\alpha_f = \frac{f_s^{max} - f_s^{min}}{f_m^{max} - f_m^{min}} \tag{15}$$

in order to overcome the limited resolution and largely environmental disturbance in micro/nano scale manipulation.

In our case, $x_m^{max} - x_m^{min} = 400\mu m$, and $x_s^{max} - x_s^{min} = 10cm$. We set $f_m^{max} - f_m^{min}$ to be $10\mu N$, and $f_s^{max} - f_s^{min}$ to be $8.46N$ based on the range of forces displayable via a SensAble PHANToM premium 1.5/6DOF haptic device [16]. Thus, we have the scaling factors $\alpha_f = 8.46 \cdot 10^5$ and $\alpha_x = 250.0$.

B. Experiment Results

Fig. 9 shows the snapshots of a successful virtual fiber-ferrule insertion of our simulation. The world coordinate system is set at the center of the workspace, with x-axis pointing right, y-axis pointing up, and z-axis pointing out.

Fig. 10 shows some experimental results obtained in one successful virtual insertion. The human operator virtually held the fiber and inserted it through the fixed ferrule from right to left with the speed, after scaled down back to the micro/nano scale, first increased from 0 to $8\mu m/s$ then decreased back to 0. The horizontal data line in Fig. 10 (bottom) shows that the non-contact forces (after being scaled down: $F_y \sim -1.2\mu N$) were in charge of the dynamics of the insertion most of the time, and the scattered data dots indicate that the contact force (after being scaled down: $F_y \in -5 \sim -10\mu N$) played major role at the end of this insertion where the user tried to keep the fiber tightly on the inner surface of the ferrule. The velocities along y and z directions are not shown in this figure, where both v_y and v_z oscillate slightly around 0 in the range of $-2\mu m/s \sim 2\mu m/s$, indicating that the movement is mainly along the $-x$ direction.

Our simulator for fiber-ferrule insertion in a virtual environment can be used to facilitate eventual automation of such micro/nano-scale optical fiber assembly. In order to have automated insertion in spite of uncertainties, it is useful to know how to correlate the force feedback to the correction of insertion motion. With our simulator, a human operator can be trained to be skillful at the magnified fiber-ferrule insertion, and his/her insertion skill can be captured in terms of insertion velocity as a function of reaction force at different time and location during insertion. Such skill could be further transferred back to the micro/nano-scale via the scaling factors and used to build a learning-based controller for automated micro/nano-scale optical fiber assembly.

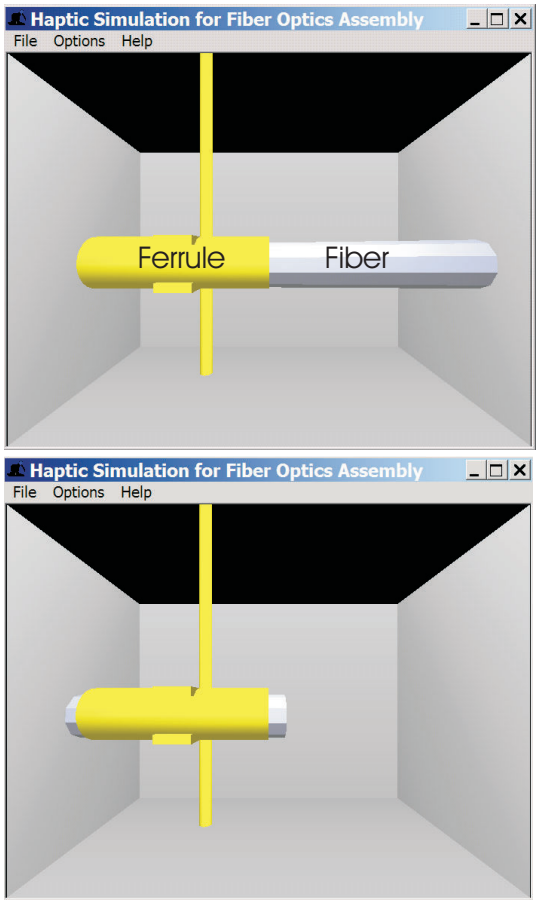

Fig. 9. Simulation of fiber-ferrule insertion

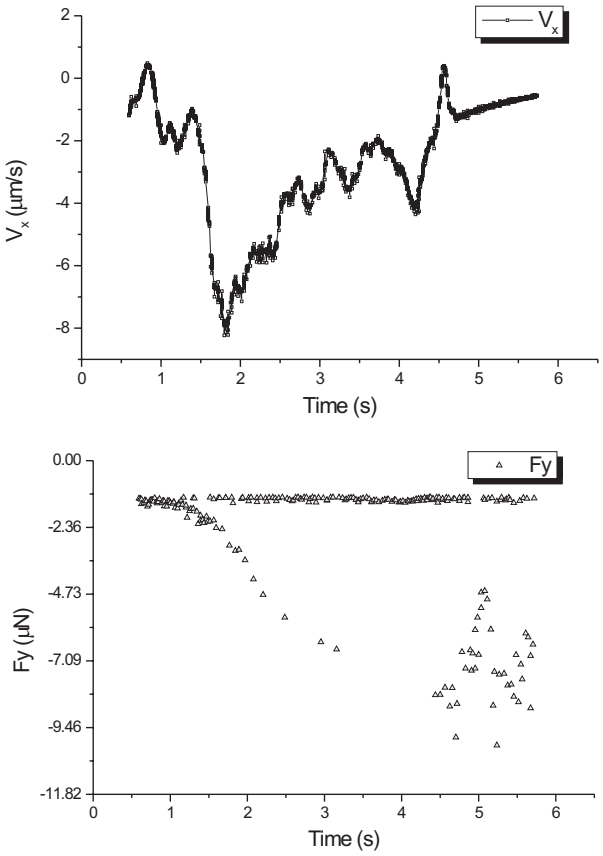

Fig. 10. Experimental results in one insertion

V. Conclusion

In this paper, we studied the force models for the step of micro/nano-scale fiber-ferrule insertion in optical fiber assembly. Different contact and non-contact forces are modeled and simulated in a virtual environment via a haptic device, which offers the operator both visual feedback and haptic feedback. The models and simulation could be useful for skill training and design of automated assembly.

The next step of this research is to extend the simulation scope to cover the complete joining step and the positioning step in the optical fiber assembly.

VI. Acknowledgement

This work is partially supported by the National Science Foundation Grants EIA-0224423 and IIS-0328782.

References

[1] A. Weber, *Assembly Handbook: Fiber Optics*. Assembly Magazine, Feb. 2002.

[2] M. Sitti, "Nsf workshop on future directions in nano-scale systems, dynamics and control," in *Automatic Control Conference (ACC)*, June 2003.

[3] M. Sitti and H. Hashimoto, "Teleoperated touch feedback from the surfaces at the nanoscale: Modeling and experiments," *IEEE/ASME Trans. on Mechatronics*, vol. 8, pp. 287–298, June 2003.

[4] G. Sharma, C. Mavroidis, and A. Ferreira, *Handbook of Theoretical and Computational Nanotechnology*, ch. 40. Virtual Reality and Haptics in Nano- and Bionanotechnology. American Scientific Publishers, 2005.

[5] H. Chen, N. Xi, G. Li, J. Zhang, and M. Prokos, "Planning and control for automated nanorobotic assembly," in *Proc. of IEEE Int. Conf. on Robotics and Automation*, (Barcelona, Spain), pp. 170–175, April 2005.

[6] M. Guthold, "Controlled manipulation of molecular samples with the nano-manipulator," *IEEE/ASME Transactions on Mechatronics*, vol. 5, no. 2, pp. 189–198, 2000.

[7] R. Colton, "Nanoscale measurements and manipulation," *J. Vac. Sci. Technol. B*, vol. 22, pp. 1609–1635, Jul/Aug 2004.

[8] *Assembly Instructions for LC Fiber Optic Jumper Connectors*. No. 640-252-054, SYSTIMAX Solutions, July 2004.

[9] N. Burnham and A. Kulik, *Handbook of Micro/Nanotribology*, ch. 5. Surface Forces and Adhesion. Boca Raton: CRC Press LLC, 1999.

[10] R. Fearing, "Survey of sticking effects for micro-parts," in *IEEE Int. Conf. on Robotics and Intelligent Systems (IROS)*, pp. 2212–2217, 1995.

[11] K. Kendall, "Adhesion: Molecules and mechanics," *Science*, pp. 1720–1725, March 1994.

[12] A. Powell and J. Warren and C. Bailey, "Mechanism of Motion of an Optical Fiber Aligned by a Solder Droplet," in *MRS Symp. Proc. 531*, pp. 95–100, April 1998.

[13] N. Tas, P. Mela, T. Krammer, J. Berenschot, and A. van den Berg, "Water plugs in nanochannels under nagative pressure," in *7th Internat onal Conference on Miniaturized Chemical and Blochemlcal Analysts Systems*, (Squaw Valley, Callfornla USA), pp. 13–16, October 5-9 2003.

[14] G. G. Adams, S. *Müftü*, and N. M. Azhar, "A nano-scale multi-asperity contact and friction model," *ASME Journal of Tribology*, vol. 125, pp. 700–708, 2003.

[15] J. Marian, B. D. Wirth, and J. M. Perlado, "Mechanism of formation and growth of $<$ 100 $>$ interstitial loops in ferritic materials," *Phys. Rev. Lett. 88, 255507*, vol. 88, pp. 1–4, June 2002.

[16] *PHANToM Premium 1.5/6DOF User's Guide*. No. 02120, SensAble Technologies, Inc., Jan. 2001.